N-DOPED NIOBIUM ACCELERATING CAVITIES: ANALYZING MODEL APPLICABILITY

W. Weingarten†, retiree from CERN, Geneva, Switzerland
R. Eichhorn, N. Stillin, Cornell Laboratory for Accelerator-Based Sciences and Education, Ithaca, NY, USA

Abstract

The goal of this research was to analyse data from multiple cavities in order to test the viability of a model for surface resistance proposed previously. The model intends to describe the behaviour of the quality factor with respect to the RF field strength, while exploring the physical cause of this phenomenon; the model is pretty general, but will be checked here specifically for N-doped niobium cavities. The data were obtained from two single-cell 1.3 GHz cavities manufactured and tested at Jefferson Lab in Newport News, VA, USA.

INTRODUCTION

The slope of the quality factor Q of superconducting (sc) cavities in dependence of the accelerating gradient E, Q(E), is still a subject of debate. Several models were presented, thereof most based on a homogeneous surface and field dependent parameters.

Instead, here a model is further investigated that involves a composite surface of a homogeneous superconductor with embedded tiny weak sc defects of size comparable to the coherence length, from now on simply called “defects”.

IMPURITY BASED MODEL

Our model which we will apply to the data has been partially published before [1,2]. It is based on the following assumptions, derived from many experimental data:

i. The RF losses of a sc niobium cavity are generated by a composite from at least two origins, a pure niobium host surface with embedded defects. Their number depends on the temperature and the RF magnetic field.
ii. These defects are themselves compounds of various purity of niobium and its alloys.
iii. The transition to the normal conducting (nc) state of the defects occurs, by the proximity effect, at relatively low RF magnetic fields and relatively low critical temperatures, as compared to the critical field and critical temperature of pure niobium.
iv. A distinction is made for defects at the surface and those in the bulk. When a defect at the surface becomes nc, the RF field shifts deeper into the bulk. When a defect in the bulk becomes nc, the RF field does not penetrate deeper.
v. With growing magnetic field, the defects become nc; this increases the RF losses at the surface and reduces the RF losses in the bulk.
    a. The increase of RF losses at the surface originates from entry of magnetic flux enlarging the number of nc electrons.
    b. The decrease of RF losses in the bulk arises from the lowering of the mean free path of the nc electrons, when the cutting edge of defects having already passed to the nc state penetrates deeper into the bulk. Their number increases logarithmically with the magnetic field (exactly valid only for a defect density constant with depth).
vi. Above a distinct temperature (~2K), the defects, when they become nc, show enlarged RF losses. The physical reason is still unclear. Possible explanations proposed are percolation [1,2] and larger thermal impedance from the transition of the liquid helium from the superfluid to the normal fluid state [3].

To analyse the new data we use the plain ansatz as suggested by [1,2] describing a temperature independent defect density without percolation.

The significance of the different terms in relation to the preceding statements (i) – (vi) is indicated in (1). The function f(B) gives the fraction of defects already undergone nc and is chosen to unity for B=B’ (at the maximum Q-value), because all defects are supposed to be nc there. The variables as used in (1) are explained in Tab. 1.

$$R_s = \left(\overbrace{A \cdot \frac{e^{-(\Delta/T)}}{T} + R_{res}}^{\substack{BCS\ and\ residual \\ surface\ resistance}} \right) - \overbrace{\left(\underbrace{A \cdot \frac{e^{-(\Delta/T)}}{T} + R_{res}}_{temperature\ dependent\ factor} \right) \cdot \underbrace{[f(B) - L_2/L_1 \cdot f(B)]}_{field\ dependent\ factor}}^{\substack{contribution\ to\ surface\ resistance \\ from\ defects\ in\ bulk}} + \overbrace{R_{s1} \cdot (-\kappa^{-2}) \left\{ 1 + \frac{\ln\left[1 - \left(\frac{\kappa B}{B_C}\right)^2\right]}{\left(\frac{\kappa B}{B_C}\right)^2} \right\}}^{\substack{contribution\ to\ surface\ resistance \\ from\ defects\ on\ surface}} \quad (1)$$

$$f(B) = \begin{cases} \dfrac{\ln(B/B_C^*)}{\ln(B'/B_C^*)}, B \geq B_C^* \\ 0, B < B_C^* \end{cases}$$

By fitting the data, it turned out that χ^2 could be reduced by supplementing these relations by a temperature dependence of the critical field B_c^* of the defect in the bulk:

$$B_C^*(T, T'^*, B_{C0}^*) = B_{C0}^* \cdot [1 - (T/T'^*)^2] \cdot \Theta(T'^* - T) \quad (2)$$

† wolfgangweingarten@cern.ch

Table 1: Variables as Used in Eqs. (1) and (2)

A	Material and frequency dependent parameter
Δ	Energy gap of niobium
R_{res}	Residual resistance
B	Maximum RF surface magnetic field
B_c	Critical magnetic field of niobium
B_{c0}^*	Critical magnetic field of defect at T=0K
T	Temperature of lHe bath
T'*	Critical temperature of defect in the bulk
L_2/L_1	Ratio of mean free paths at field associated with maximum Q and at low field
R_{s1}	Contribution to surface resistance from defects on surface
κ	Ginzburg-Landau parameter

The relevant parameters for the surface resistance R_s are the penetration depth λ and the conductivity σ,

$$R_s = (1/2)\mu_0\omega^2\lambda^3\sigma,$$

both depending on the mean free path L and the temperature T,

$$\lambda(T,L) = \lambda_L(T)\sqrt{\xi_0/\xi(L)} \quad ,$$

$$\lambda_L(T) = \sqrt{\frac{m}{n_s(T)e^2\mu_0}} \quad ,$$

$$\sigma(T,L) = \frac{n_n(T)e^2L}{mv_F} \quad ,$$

with

$$\xi^{-1}(L) = \xi_0^{-1} + L^{-1} .$$

λ_L is the London penetration depth, ξ the coherence length, ξ_0 the coherence length of pure niobium, v_F the Fermi velocity, n_s the density of sc electrons, n_n that of the nc electrons, m the effective electron mass, and ω the RF frequency.

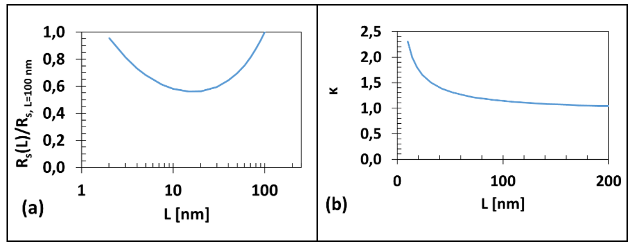

Figure 1: Dependence on L of (a) the ratio of R_s at B-field optimum and low B and of (b) the Ginzburg-Landau parameter κ.

The "BCS" surface resistance, as derived from the two-fluid model, then becomes [4]

$$R_{s,BCS} = (1/2)\mu_0\omega^2\lambda_L^3(T)\sigma(T,L)\xi_0^{3/2}(\xi_0^{-1}+L^{-1})^{3/2} . \quad (3)$$

Two cases can be distinguished from (3) depending if L is large or small compared to $_0/2$. As the electrical conductivity σ of the nc electrons is proportional to L, the surface resistance is either

$$R_s \sim L \;(L \gg \xi_0/2)$$

or

$$R_s \sim 1/\sqrt{L} \;(L \ll \xi_0/2) \quad .$$

The minimum of R_s hence lies at $\xi_0/2$ (ξ_0=33 nm for niobium). As for standard sc accelerating cavities in general, and for the nitrogen doped cavities, too, L is larger

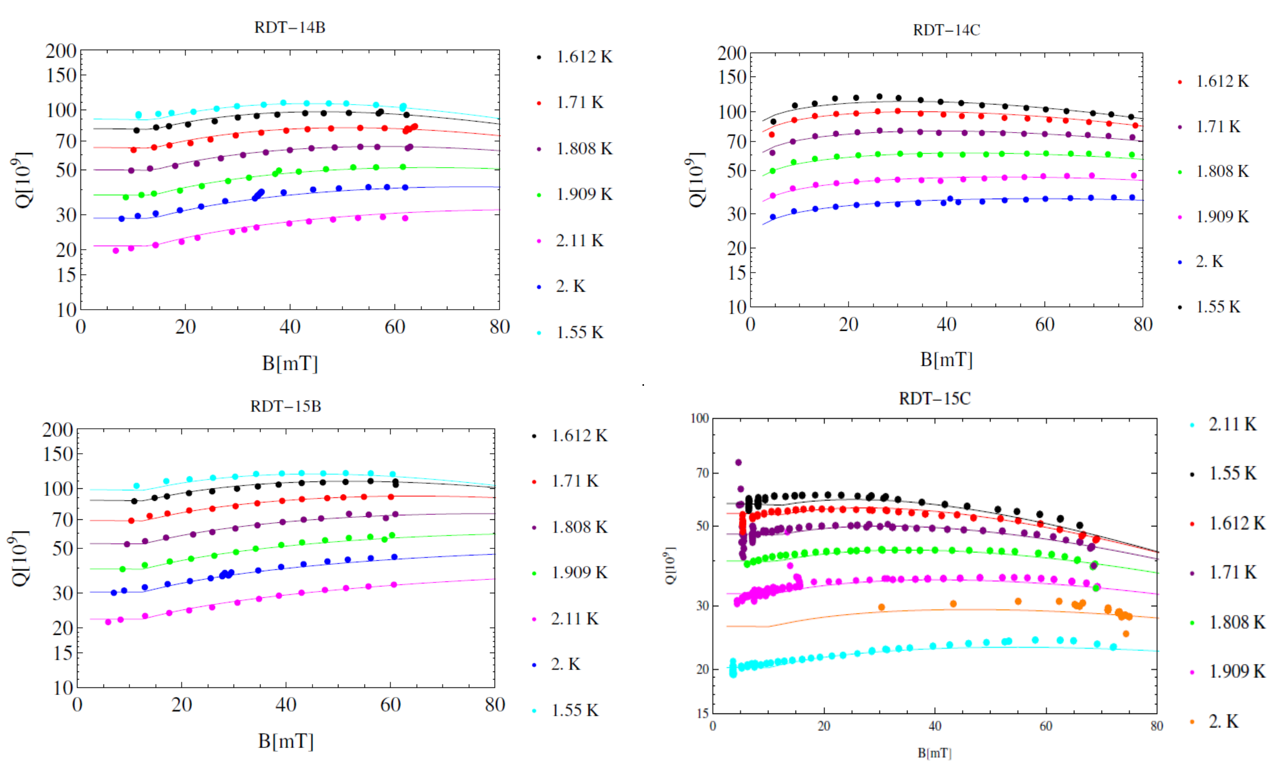

Figure 2: Q values versus peak magnetic surface field for the 4 cavities under study.

ISBN 978-3-95450-169-4

Table 2: Results of fit. 180/20N/10+15µm EP means: 180 minutes @ 800°C in vacuum, 20 minutes of exposure to N2 at 800°C, 10 minutes with vacuum again @ 800°C, 15 µm Electro-Polishing (EP).

item	unit	RDT-14B	RDT-14C	RDT-15B	RDT-15C
treatment	-	180/20N/10+ 15µm EP	180/20N/10+55µm EP+180/2N/60+10µm EP	180/20N/50+ 15µm EP	180/3N/60+10 µm EP
# data	-	115	110	105	931
χ^2	-	51	48	27	999
A	nΩK	$(95\pm3)\cdot10^3$	$(90\pm4)\cdot10^3$	$(79\pm2)\cdot10^3$	$(109\pm11)\cdot10^3$
Δ	K	17.6±0.1	17.0±0.1	17.30±0.05	18.2±0.2
R_{res}	nΩ	2.3±0.1	2.4±0.15	2.0±0.1	4.3±0.3
B_{c0}^*	mT	14±3	<2	16.3±1.5	15±10
R_{s1}	nΩ	16±3	12±2	14±3	30±8
L_2/L_1	-	0.63±0.02	0.59±0.03	0.30±0.03	0.61±0.09
T'*	K	>5	>3	>6.5	>3
κ	-	<1.8	<1.5	<1.8	<1.8
B_c	mT	200±20	200±25	200±30	200±30
B'	mT	60±10	90±20	200±30	>120
R_{BCS} (2 K, 1.3 GHz, $B<B_{c0}$*)	nΩ	7.2±0.6	8.8±0.5	7.0±0.3	6.6±1.6
$\Delta/(k_BT_c)$	-	1.90±0.01	1.84±0.01	1.87±0.01	1.95±0.03
Mean free path L_2 (from κ)	nm	>19	>32	>20	>20
Mean free path L_2 (from L_2/L_1)	nm	20±10	20±10	5-60	4-60
Mean free path L_1 (from L_2/L_1)	nm	84±6	92±8	235±25	100±30

than $\xi_0/2$, the choice of L_2/L_1 as a relevant parameter in (1) is justified. Figure 1(a) displays the minimum of the ratio of the surface resistances $R_s(L)/R_{s,L=100\ nm}$.

The data were obtained on 1.3 GHz mono-cell niobium cavities made available to us from Jefferson Lab, Newport News, VA, USA. The Q vs B curves are shown in Figure 2. The characteristic features of these cavities were B/E=4.31, G=$R_s\cdot Q$=277 Ω. The results of the fitting are summarized in Table 2, top. The error limits are taken from twice the minimum of χ^2. For cavity "RDT-14C" two data sets (~2K) stuck out of the remainder and were therefore left out. After this the goodness of fits χ^2 lies below the number of data points, as it should be, except for cavity "RDT-15C" with its χ^2 slightly above. This cavity had undergone a relatively short N-doping (3 minutes) compared with the other three. All fitted parameters are in a physically sensible range.

The model of (1,2) provides a handle for understanding better the physics of N-doping by virtue of the Ginzburg-Landau parameter κ and the ratio L_2/L_1 of the mean free paths at maximum Q-value and low field Q-value. The parameter κ depends on the mean free path L according to the relation [5]

$$\kappa = \frac{2\sqrt{3}}{\pi}\cdot\frac{\lambda_L\sqrt{1+\frac{\pi\xi_0}{2L}}}{\xi_0\left[1+\left(\frac{T}{T_c}\right)^2\right]} \quad , \tag{4}$$

which is displayed in Figure 1(b) for niobium with ξ_0=33 nm, λ_L=29 nm and T_c=9.25 K as typical numbers. The range for L_2, as derived from (3), stretches from >19 to >32 (Table 2, bottom). This is close or above the theoretical minimum for the surface resistance at $\xi_0/2$.

By virtue of (3), the ratio L_2/L_1 allows a second estimation of the mean free path L_2 at optimum Q-value and of the mean free path L_1 at low field (Table 2, bottom).

In conclusion, the benefits of N-doping are caused by the logarithmic reduction with the magnetic field of the mean free path from about 100-200 nm at low field down towards the theoretical minimum. The new data hence confirm the model as presented in [2]. These findings were substantiated elsewhere, too [6,7].

ACKNOWLEDGEMENTS

The authors are very much obliged to Dr. Charles Reece from Jefferson Lab for providing us with the data analysed here. One of us (WW) also likes to thank the staff of CLASSE, Cornell University, and in particular Michael Roman, for making available Cornell's computer facilities to perform the data analysis with Mathematica® from his home in Europe.

REFERENCES

[1] W. Weingarten, *Phys. Rev. Special Topics - Accelerators and Beams* ***14*** (2011) 101002.

[2] W. Weingarten and R. Eichhorn, in *Proceedings of SRF2015*, Whistler, BC, Canada (2015) p. 95.

[3] G. Ciovati, P. Dhakal, and A. Gurevich, *Applied Physics Letters* ***104*** (2014) 092691.

[4] W. Weingarten, *Particle World* ***1*** (1990) p. 93.

[5] T. Junginger, PhD thesis 2013, University of Heidelberg (Germany), *EuCARD Editorial Series on Accelerator Science and Technology* (J - P.Koutchouk, R.S.Romaniuk, Editors), Vol.15, p. 28.

[6] P. Dhakal, G. Ciovati, P. Kneisel, and G. R. Myneni, *Proceedings of IPAC2015*, Richmond, VA, USA (2015) 3506.

[7] J. T. Maniscalco, D. Gonnella, and M. Liepe, arXiv:1607.01411v2, 5 Aug 2016.